Development of Background-Limited MKID Systems for Millimeter-Wave and Far-Infrared Observations

J. Austermann[1], J. Beall[1], D. Becker[1], H.-M. Cho[2], M. Devlin[3], B. Dober[3], S. Duff[1], J. Gao[1], C. Groppi[4], G.C. Hilton[1], J. Hubmayr[1], K.D. Irwin[2], D. Li[1], P. Mauskopf[4], D.P Pappas[1], L. Vale[1], J. Van Lanen[1], M.R. Vissers[1], Y. Wang[1,5],

[1]*National Institute of Standards and Technology, Boulder, CO 80305, USA*

[2]*Stanford University, Department of Physics, Stanford, CA 94305, USA*

[3]*University of Pennsylvania, Department of Physics & Astronomy, 209 South 33rd St, Philadelphia, PA 19104, USA*

[4]*Arizona State University, School of Earth & Space Exploration, 781 S Terrace Rd, Tempe, AZ 85281,USA*

[5]*Southwest Jiaotong University, Quantum Optoelectronics Laboratory, Chengdu, China*

*Contact: Jason.Austermann@nist.gov, phone +1-303-497-4785

***Abstract*—NIST-Boulder is heading a program in the development of feedhorn-coupled, background-limited Microwave Kinetic Inductance Detectors (MKIDs) for observation at far-infrared to millimeter wavelengths. MKIDs provide a compelling path forward towards the next generation of large-format polarimeters, imagers, and spectrometers for experiments in cosmology and astrophysics that will require channel counts on order 10,000. Here we present performance results of our latest devices being developed for the sub-orbital, next generation BLAST polarimeter experiment that will operate in bandpasses centered at 600, 850, and 1200 GHz. We will review major recent milestones, including background-limited performance in the prototype BLAST 1.2 THz pixels over a wide range of input powers relevant to both balloon-borne and satellite experiments. We also review efforts at NIST to expand this technology to a wide range of applications through scaling to various frequencies (150 GHz – 1.4 THz), coupling techniques, multi-frequency pixels, material development, and readout development that will allow for a high level of scalability.**

I. Introduction

Microwave Kinetic Inductance Detectors (MKIDs) are superconductor microresonators that absorb and detect coupled radiation through the breaking of Cooper pairs in the superconductor. When designed as a high quality factor resonator, MKIDs naturally serve as both the detector and a multiplexing circuit in the frequency domain. Together with their typically simple fabrication, this makes MKIDs an attractive option for the next generation of large-format detector arrays in the far-infrared and (sub-)millimeter experiments. MKIDs have a broad range of applications, including several experiments recently fielded or under development for continuum [1]–[3], polarimetry [4], or spectroscopic observations [5]–[7].

MKID sensitivity has improved by orders of magnitude since inception [8] through superconductor material development, improved coupling efficiency, and design geometries that all work to reduce intrinsic detector noise and increase responsivity. However, for many applications, significant additional improvements in performance are needed for MKIDs to match the background-limited sensitivity performance and array uniformity offered by established alternative detector technologies, e.g. the transition edge sensor (TES). Here, we describe our program and progress in developing highly scalable end-to-end MKID solutions that will meet the requirements of the next generation of experiments. We review the critical aspects of our MKID and experimental design, and report on the latest performance measurements and results, including the successful production of background-limited MKID polarimeters operating in the 1.2 THz band at low incident powers that are relevant to satellite and balloon-borne experiments [9].

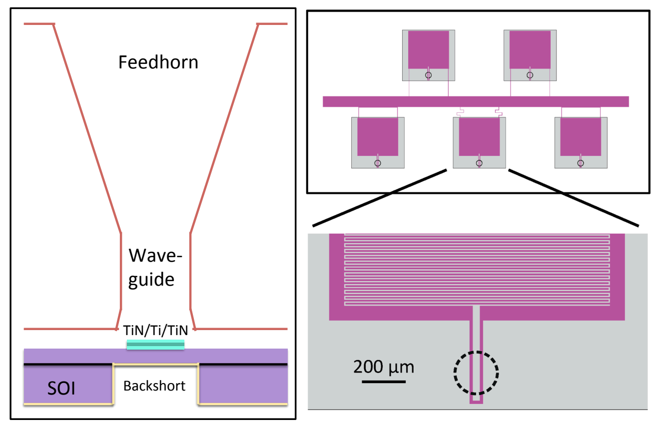

Fig. 1. Feedhorn-coupled kinetic inductance polarimeter concept and prototype design. Left: Cross-section schematic of primary device layers and feedhorn/waveguide coupling scheme (not to scale). Right: Prototype chip design with a common microstrip feedline coupled to five lumped-element resonators. Grey squares outline the area of the backside silicon etch that creates the quarter-wave backshort. Zoom-in view depicts a single pixel comprising a single turn inductor and a 5 μm spacing IDC. The dashed-circle represents the approximate position and diameter of the feedhorn's exit waveguide.

II. MKID Design

MKIDs work on the basic principle of using photons to break cooper pairs in a superconductor. When built as a super-

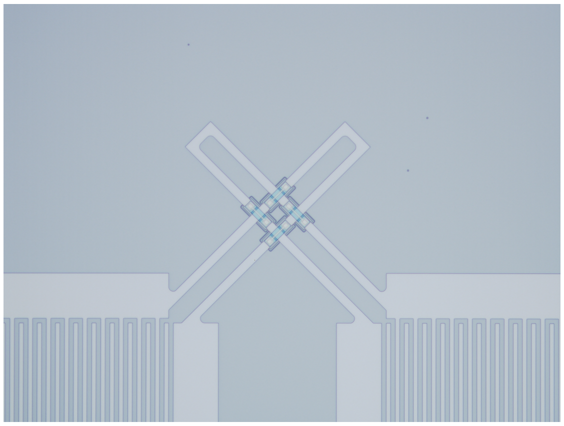

Fig. 2. Photograph of absorber inductor strips in a prototype dual-polarization pixel, designed specifically for the verification and testing of the insulated crossover schemes.

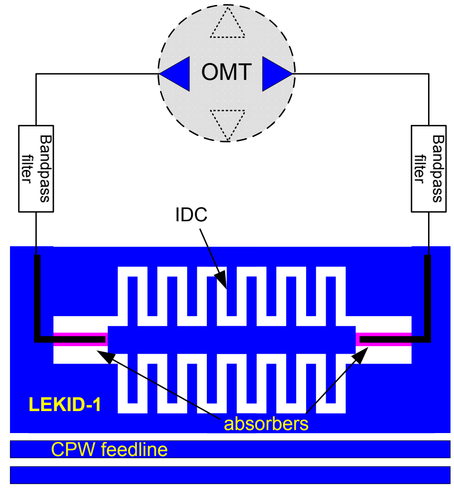

Fig. 3. Concept of an MKID-based dual-polarization pixel coupled via a planar ortho-mode transducer (OMT) Components of the second polarization channel are omitted for simplicity. Radiation is coupled via feedhorn and waveguide directly to the OMT. A Nb ground plane is depicted in blue. Nb microstrip (black) on top of TiN/Ti/TiN (red) forms a lossy transmission line that absorbs the radiation from the OMT. The large IDC capacitively couples the MKID to the coplanar waveguide (CPW) feedline.

conducting resonator, the resulting change in the quasiparticle density affects both the circuit's quality factor and resonant frequency. With high quality factors, many devices can be measured simultaneously off a common feed line – one of the primary attractions of MKIDs is the potential reduction of both cost and complexity as the next generation of experiments move to order 10^4 channels.

A. Detector Design

The basic concept of our MKID design is outlined in Fig. 1. The resonant circuit is fabricated from a single TiN/Ti/TiN trilayer. Incident radiation couples to an inductive strip that serves as both the polarization-sensitive absorber and the inductive component of the microwave resonant circuit. A lithographed on-chip Interdigitated Capacitor (IDC) completes the resonant circuit. A quarter-wave backshort maximizes coupling efficiency and is fabricated to the correct depth through backside etching of a silicon-on-insulator (SOI) wafer and a conductor deposited on the back surface.

Our TiN/Ti/TiN trilayer films exhibit many properties that can be advantageous compared to traditional MKID superconductor materials. The trilayer T_c can be tuned between $\sim$800 mK and 3 K [10], which allows the MKID to be optimized for the specific observation wavelength(s), optical loading, and bath temperature of the application. The trilayer also produces highly uniform T_c, with $< 1.5\%$ variation across a 75 mm wafer [10], which is critical for scaling to large format MKID arrays (e.g. 150 mm diameter wafers) with optimized performance. A high sheet resistance allows for convenient waveguide impedance matching, while the trilayer's relatively high kinetic inductance fraction helps maximize responsivity. The TiN/Ti/TiN trilayer exhibits a linear frequency response with optical power (see Sec. III) that doubles the responsivity with respect to conventional superconductors. The trilayer also has low two-level system (TLS) noise properties due to the low TLS density of the TiN-Si interface [11], [12]. Additionally, the large kinetic inductance of the trilayer decreases the resonator frequency into the $\hbar\omega \ll k_{\mathrm{B}}T$ regime, which reduce the TLS noise through the TLS saturation effect [13], [14].

B. Optical Coupling

As with other detector technologies at these frequencies, several different optical coupling schemes have traditionally been employed to couple photons to the MKID absorber, including antenna, microlens, feedhorn, and/or direct absorber. We have chosen to couple the radiation to each detector via feedhorn and waveguide (see Fig. 1), which has several advantages including: (i) increased inter-pixel spacing allowing use of large interdigitated capacitors (IDCs) to minimize TLS noise and pixel crosstalk; (ii) high absorption efficiency and low coupling to stray light; (iii) concentrated light decreases detector volume and increases detector responsivity; (iv) excellent polarization properties; and (v) near Gaussian-shaped beams. NIST's silicon platelet feedhorn technology [15] provide a scalable corrugated feed solution that is well matched to the silicon detector array.

In the currently presented design, the feedhorn couples radiation directly to the inductor strip of a single-polarization MKID. We are now developing dual-polarization pixels using two MKIDs with cross-over orthogonal inductor strips (Fig. 2). We are also exploring coupling radiation to a planar ortho-mode transducer (OMT) that separates signals in the two linear polarizations onto superconducting microstrips, as depicted in Fig. 3. Planar OMT coupling is a mature technology [16], [17] that has already been deployed in several TES-based experiments , including SPTpol [18], ACTPol [19], and the Atacama B-mode Search (ABS) [20]. Use of an OMT

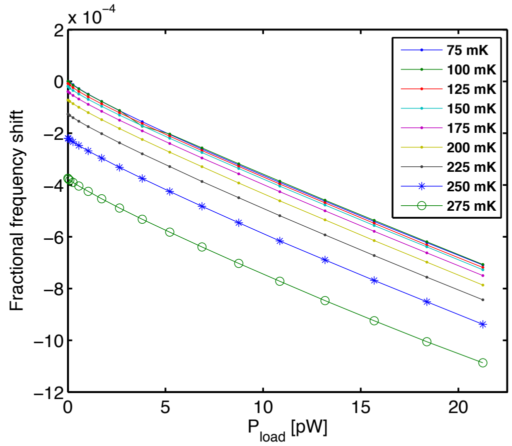

Fig. 4. Detector responsivity shown as fractional frequency shift verses the optical loading power measured at different bath temperatures.

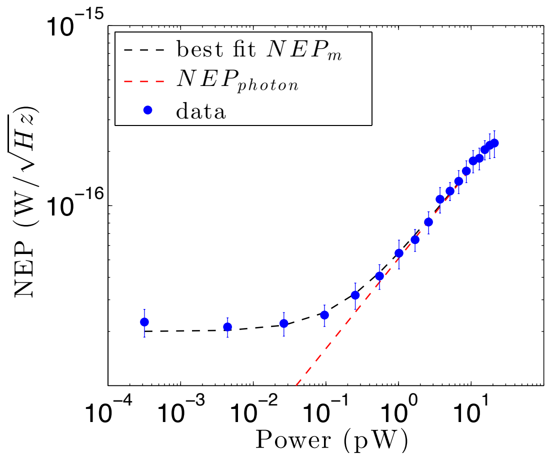

Fig. 5. Detector noise equivalent power (NEP) as a function of optical load power. Measured NEP (points) at optical powers above $\geq$ 0.5 pW are in good agreement with the photon-noise prediction (red-dashed). The black-dashed line represents the best fit NEP model defined in Eq. 1. This plot is reproduced, with permission, from [9].

also has the advantage of separating the coupling from the absorbing inductor, thus adding flexibility in the geometric maximization of responsivity. Passbands are currently defined through the combined use of free-space low-pass filters in front of the feedhorns and the high-pass cutoff provided by the waveguide. Furthermore, use of an OMT would allow the signal from a wide-bandwidth feedhorn to be partitioned into several observation frequency bands using on-chip filters (e.g. [21].

III. PERFORMANCE RESULTS

We report on the latest measurements, characterizations, and performance milestones of our MKID devices. We include a review of experimental design and measurement techniques. Initial results are from the prototype single-polarization 5-channel devices depicted in Fig. 1, which are feedhorn-coupled to a $\Delta\nu \approx 400$ GHz passband centered at $\nu \approx 1.2$ THz.

A. Linear Response

Measurements are made using a homodyne measurement and cryogenic SiGe amplifier. The detectors are exposed to radiative loads between 0.3 fW and 21 pW using a variable temperature blackbody load. A frequency sweep and fit to the complex transmission $S_{21}(f)$ yields the resonant frequency as a function of radiative loading. We observe a fractional frequency shift, $\delta f/f$, that is linear with optical power and has an approximately constant slope with bath temperature (Fig. 4). Conventional superconducting materials typically have a response of $\delta f/\delta P \propto P^{-0.5}$, therefore, the approximately linear response shown in Fig. 4 represents a significant departure from this behavior. Similar characteristics have been seen previously in TiN films [22], [23], thus representing an advantage of TiN based films and trilayers. The linear response of these films is not yet fully understood, and we will discuss our latest measurements and experiments to understand the observed behavior of these materials.

B. Photon-Limited Performance at 1.2 THz

The fundamental sensitivity limit of any integrating photon power detector is determined by the photon-rate fluctuations from the emitting source under observation. This is often referred to as the photon-noise limit or background limit. We directly measure the fractional frequency noise of the resonators at each radiative load level. Using the measured responsivity of the resonator (e.g. Fig. 4), we convert the measured white-noise level to a noise equivalent power (NEP) and compare it to expected noise level from known sources at each optical loading power. The results are shown in Fig. 5 and represent a major milestone of this project: *photon-noise limited sensitivity down to loading powers* $\geq$ *0.5 pW*. Details of these measurements and result can be found in [9].

Fig. 5 also shows the full data set fit to the model

$$NEP_m^2 = NEP_\alpha^2 + \frac{NEP_{photon}^2 + NEP_R^2}{\eta}, \quad (1)$$

where NEP_{photon} is the predicted photon noise (red-dashed line) and NEP_R is the quasiparticle recombination noise, which is sub-dominant when the photon energy is significantly larger than the superconducting energy gap. The free parameters are η, the total optical efficiency, and NEP_α, a constant term representing the combined device and experimental noise floor. The fit yields $\eta = 0.69 \pm 0.01$ and $NEP_\alpha = 2 \times 10^{-17}$ W/$\sqrt{\text{Hz}}$ [9].

C. Ongoing Measurements

We will also present the latest detector characterization measurements compared to modeling results and expectations. This will include mapping of beam properties using a chopped blackbody source on an x/y translation stage and polarimeter characterization using a chopped source and rotating polarizing wire grid. Initial polarization measurements of the prototype single-polarization MKIDs match the co-polar (η_c) and cross-polar (η_x) efficiencies derived from electromagnetic coupling simulations. Similar models of a modified prototype design suggest $\eta_c \sim 0.8$ and $\eta_x \leq 0.02$ are achievable.

IV. Future Work

Future MKID design iterations will include dual-polarization pixels and OMT coupled MKIDs with on-chip band defining filters. We will also be scaling these designs to operate in other frequency bands, including large-format arrays at 600 GHz, 850 GHz, and 1.2 THz for the next-generation BLAST polarimeter, while striving to maintain photon-limited performance by maximizing responsivity and minimizing inherent detector noise sources. We will also begin incorporating a multiplexing readout scheme using NIST developed SiGe amplifiers and ROACH based digital readout modules [24], which together will allow the readout of ~1000 MKIDs per amplifier/module.

V. Conclusion

We have undertaken an MKID development program to produce and end-to-end MKID solution for background limited mm/sub-mm/THz imaging and polarimetry, including all necessary elements from optical coupling through warm read out. Through the benefits of feedhorn-coupling and the use of a TiN/Ti/TiN trilayer superconducting film, we have produced a photon-noise limited MKID-based polarimeter solution in the 1.2 THz band at incident powers that are relevant for balloon-based and satellite experiments. Near-term development includes dual-polarization pixel arrays, scaling of designs to operate at lower frequency bands, and the integration of scalable multiplexing readout components.

References

[1] S. R. Golwala, C. Bockstiegel, S. Brugger, N. G. Czakon *et al.*, “Status of MUSIC, the MUltiwavelength Sub/millimeter Inductance Camera,” vol. 8452, Sep. 2012.

[2] A. Monfardini, R. Adam, A. Adane, P. Ade *et al.*, “Latest NIKA Results and the NIKA-2 Project,” Dec. 2013.

[3] L. J. Swenson, P. K. Day, C. D. Dowell, B. H. Eom *et al.*, “MAKO: a pathfinder instrument for on-sky demonstration of low-cost 350 micron imaging arrays,” vol. 8452, Sep. 2012.

[4] J. Hubmayr, J. Beall, D. Becker, J. Brevik *et al.*, “Dual-polarization-sensitive kinetic inductance detectors for balloon-borne sub-millimeter polarimetry,” *accepted in Journal of Low Temperature Physics*, 2014.

[5] E. Shirokoff, P. S. Barry, C. M. Bradford, G. Chattopadhyay *et al.*, “MKID development for SuperSpec: an on-chip, mm-wave, filter-bank spectrometer,” vol. 8452, Sep. 2012.

[6] A. Endo, J. J. A. Baselmans, P. P. van der Werf, B. Knoors *et al.*, “Development of DESHIMA: a redshift machine based on a superconducting on-chip filterbank,” vol. 8452, Sep. 2012.

[7] G. Cataldo, W.-T. Hsieh, W.-C. Huang, S. H. Moseley, T. R. Stevenson, and E. J. Wollack, “Micro-Spec: an ultracompact, high-sensitivity spectrometer for far-infrared and submillimeter astronomy,” *Appl. Opt.*, vol. 53, p. 1094, Feb. 2014.

[8] P. K. Day, H. G. LeDuc, B. A. Mazin, A. Vayonakis, and J. Zmuidzinas, “A broadband superconducting detector suitable for use in large arrays,” vol. 425, pp. 817–821, Oct. 2003.

[9] J. Hubmayr, D. Becker, M. Devlin, B. Dober *et al.*, “Demonstration of photon-noise limited sensitivity in feedhorn-coupled kinetic inductance detectors,” submitted.

[10] M. R. Vissers, J. Gao, M. Sandberg, S. M. Duff, D. S. Wisbey, K. D. Irwin, and D. P. Pappas, “Proximity-coupled Ti/TiN multilayers for use in kinetic inductance detectors,” *Applied Physics Letters*, vol. 102, no. 23, p. 232603, Jun. 2013.

[11] R. M. J. Janssen, J. J. A. Baselmans, A. Endo, L. Ferrari, S. J. C. Yates, A. M. Baryshev, and T. M. Klapwijk, “High optical efficiency and photon noise limited sensitivity of microwave kinetic inductance detectors using phase readout,” *Applied Physics Letters*, vol. 103, no. 20, p. 203503, Nov. 2013.

[12] J. B. Chang, M. R. Vissers, A. D. Córcoles, M. Sandberg *et al.*, “Improved superconducting qubit coherence using titanium nitride,” *Applied Physics Letters*, vol. 103, no. 1, p. 012602, 2013.

[13] J. Zmuidzinas, “Superconducting microresonators: Physics and applications,” *Annual Review of Condensed Matter Physics*, vol. 3, no. 1, pp. 169–214, 2012. [Online]. Available: http://www.annualreviews.org/doi/abs/10.1146/annurev-conmatphys-020911-125022

[14] S. Kumar, J. Gao, J. Zmuidzinas, B. A. Mazin, H. G. LeDuc, and P. K. Day, “Temperature dependence of the frequency and noise of superconducting coplanar waveguide resonators,” *Applied Physics Letters*, vol. 92, no. 12, pp. 123 503–123 503, 2008.

[15] J. P. Nibarger, J. A. Beall, D. Becker, J. Britton *et al.*, “An 84 Pixel All-Silicon Corrugated Feedhorn for CMB Measurements,” *Journal of Low Temperature Physics*, Dec. 2011.

[16] K. Rostem, A. Ali, J. W. Appel, C. L. Bennett *et al.*, “Scalable background-limited polarization-sensitive detectors for mm-wave applications,” in *Society of Photo-Optical Instrumentation Engineers (SPIE) Conference Series*, ser. Society of Photo-Optical Instrumentation Engineers (SPIE) Conference Series, vol. 9153, Jul. 2014, p. 0.

[17] J. Hubmayr, J. Austermann, J. Beall, D. Becker *et al.*, “Feedhorn-Coupled Transition-Edge Superconducting Bolometer Arrays for Cosmic Microwave Background Polarimetry,” *In These Proceedings*.

[18] J. E. Austermann, K. A. Aird, J. A. Beall, D. Becker *et al.*, “SPTpol: an instrument for CMB polarization measurements with the South Pole Telescope,” in *Society of Photo-Optical Instrumentation Engineers (SPIE) Conference Series*, ser. Society of Photo-Optical Instrumentation Engineers (SPIE) Conference Series, vol. 8452, Sep. 2012.

[19] M. D. Niemack, P. A. R. Ade, J. Aguirre, F. Barrientos *et al.*, “ACTPol: a polarization-sensitive receiver for the Atacama Cosmology Telescope,” in *Society of Photo-Optical Instrumentation Engineers (SPIE) Conference Series*, ser. Society of Photo-Optical Instrumentation Engineers (SPIE) Conference Series, vol. 7741, Jul. 2010.

[20] T. Essinger-Hileman, J. W. Appel, J. A. Beall, H. M. Cho *et al.*, “The Atacama B-Mode Search: CMB Polarimetry with Transition-Edge-Sensor Bolometers,” *AIP Conference Proceedings*, vol. 1185, no. 1, pp. 494–497, 2009.

[21] J. McMahon, J. Beall, D. Becker, H. M. Cho *et al.*, “Multi-chroic Feed-Horn Coupled TES Polarimeters,” *Journal of Low Temperature Physics*, vol. 167, pp. 879–884, Jun. 2012.

[22] C. M. McKenney, H. G. Leduc, L. J. Swenson, P. K. Day, B. H. Eom, and J. Zmuidzinas, “Design considerations for a background limited 350 micron pixel array using lumped element superconducting microresonators,” vol. 8452, Sep. 2012.

[23] M. R. Vissers, J. Gao, D. S. Wisbey, D. A. Hite, C. C. Tsuei, A. D. Corcoles, M. Steffen, and D. P. Pappas, “Low loss superconducting titanium nitride coplanar waveguide resonators,” *Applied Physics Letters*, vol. 97, no. 23, p. 232509, 2010.

[24] R. Duan, S. McHugh, B. Serfass, B. A. Mazin *et al.*, “An open-source readout for mkids,” in *SPIE Astronomical Telescopes+ Instrumentation*. International Society for Optics and Photonics, 2010, pp. 77 411V–77 411V.